受入
88-2-114
高工研図書室

EUROPEAN ORGANIZATION FOR NUCLEAR RESEARCH

CERN-EP/88-06
January 18th, 1988

MEASUREMENT OF THE RATIOS OF DEEP INELASTIC MUON-NUCLEUS CROSS SECTIONS ON VARIOUS NUCLEI COMPARED TO DEUTERIUM

The European Muon Collaboration

Aachen[1], CERN[2], Freiburg[3], Heidelberg[4], Lancaster[5], LAPP (Annecy)[6], Liverpool[7], Marseille[8], Mons[9], Oxford[10], Rutherford[11], Sheffield[12], Turin[13], Uppsala[14], Warsaw[15], Wuppertal[16], Yale[17].

J. Ashman[12], B. Badelek[15a)], G. Baum[17b)], J. Beaufays[2], C.P. Bee[7], C. Benchouk[8], I.G. Bird[5c)], S.C. Brown[7d)], M.C. Caputo[17], H.W.K. Cheung[10], J. Chima[11e)], J. Ciborowski[15a)], R.W. Clifft[11], G. Coignet[6], F. Combley[12], G. Court[7], G D'Agostini[8], J. Drees[16], M. Düren[1], N. Dyce[5], A.W. Edwards[16f)], M. Edwards[11], T. Ernst[3], M.I. Ferrero[13], D. Francis[7], E. Gabathuler[7], J. Gajewski[15a)], R. Gamet[7], V. Gibson[10g)], J. Gillies[10], P. Grafström[14g)], E. Hagberg[14], K. Hamacher[16], D.v. Harrach[4], P. Hayman[7], J.R. Holt[7], V.W. Hughes[17], A. Jacholkowska[2h)], T. Jones[7i)], E.M. Kabuss[3c)], B. Korzen[16], U. Krüner[16], S. Kullander[14], U. Landgraf[3], D. Lanske[1], F. Lettenström[14], T. Lindqvist[14], M. Matthews[7], Y. Mizuno[4], K. Mönig[16], F. Montanet[8g)], J. Nassalski[15j)], T. Niinikoski[2], P.R. Norton[11], G. Oakham[11k)], R.F. Oppenheim[17l)], A.M. Osborne[2], V. Papavassiliou[17], N. Pavel[16], C. Peroni[13], H. Peschel[16], R. Piegaia[17], B. Pietrzyk[8], U. Pietrzyk[16m)], B. Povh[4], P. Renton[10], J.M. Rieubland[2], K. Rith[3c)], E. Rondio[15a)], L. Ropelewski[15a)], D. Salmon[12i)], A. Sandacz[15j)], M. Scheer[1], T. Schröder[3], K.P. Schüler[17], K. Schultze[1], T-A. Shibata[4], T. Sloan[5], A. Staiano[4n)], H.E. Stier[3], J. Stock[3], G.N. Taylor[10o)], J.C. Thompson[11], T. Walcher[4p)], S. Wheeler[12], W.S.C. Williams[10], S.J. Wimpenny[7q)], R. Windmolders[9], W.J. Womersley[10r)].

(Submitted to Physics Letters)

ABSTRACT

Results are presented on the ratios of the deep inelastic muon-nucleus cross sections for carbon, copper and tin nuclei to those measured on deuterium. The data confirm that the structure functions of the nucleon measured in nuclei are different from those measured on quasi-free nucleons in deuterium. The kinematic range of the data is such that $\langle Q^2 \rangle \sim 5$ GeV^2 at $x \sim 0.03$, increasing to $\langle Q^2 \rangle \sim 35$ GeV^2 for $x \sim 0.65$. The measured cross section ratios are less than unity for $x \lesssim 0.05$ and for $0.25 \lesssim x < 0.7$. The decrease of the ratio below unity for low x becomes larger as A increases as might be expected from nuclear shadowing. However this occurs at relatively large values of $Q^2 (\sim 5$ GeV$^2)$ indicating that such shadowing is of partonic origin.

For footnotes see next page

a) University of Warsaw, Poland.
b) Permanent address, University of Bielefeld, Germany.
c) Now at MPI für Kernphysik, Heidelberg, Germany.
d) Now at TESA S.A., Renens, Switzerland.
e) Now at British Telecom, Ipswich, England.
f) Now at Jet, Joint Undertaking, Abingdon, England.
g) Now at CERN, Geneva, Switzerland.
h) Now at L.A.L., Orsay, France.
i) Now at R.A.L., Chilton, Didcot, England.
j) Institute for Nuclear Studies, Warsaw, Poland.
k) Now at NRC, Ottawa, Canada.
l) Now at AT&T, Naperville, Illinois, U.S.A.
m) Now at MPI für Neurologische Forschung, Köln, Germany.
n) Now at INFN, Torino, Italy.
o) Now at University of Melbourne, Parkville, Australia.
p) Now at University of Mainz, Mainz, Germany.
q) Now at University of California, Riverside, U.S.A.
r) Now at University of Florida, Gainesville, U.S.A.

Addresses

1) III. Physikalisches Inst. A, Physikzentrum, Aachen, Germany.
2) CERN, Geneva, Switzerland.
3) Fakultät für Physik, Universität Freiburg, Germany.
4) Max-Planck Institute für Kernphysik, Heidelberg, Germany.
5) Department of Physics, University of Lancaster, England.
6) Laboratoire de Physique des Particules, IN2P3, Annecy-le-Vieux, France.
7) Department of Physics, University of Liverpool, England.
8) Centre de Physique des Particules, Faculté des Sciences de Luminy, Marseille, France.
9) Faculté des Sciences, Université de L'Etat à Mons, Belgium.
10) Nuclear Physics Laboratory, University of Oxford, England.
11) Rutherford-Appleton Laboratory, Chilton, Didcot, England.
12) Department of Physics, University of Sheffield, England.
13) Istituto di Fisica, Università di Torino, Italy.
14) Department of Radiation Science, University of Uppsala, Sweden.
15) Physics Institute, University of Warsaw, and Institute for Nuclear Studies, Warsaw, Poland.
16) Fachbereich Physik, Universität Wuppertal, Germany.
17) Physics Department, Yale University, New Haven, Connecticut, U.S.A.

INTRODUCTION

Prior to the presentation by the European Muon Collaboration [1] of a comparison between the nucleon structure function F_2 measured on iron and deuterium, it had generally been assumed that the deep inelastic cross section on a heavy nucleus would be given by the incoherent sum of the cross sections on the constituent nucleons, apart from the effects of the Fermi momentum of the nucleons. The cross section ratio σ^{Fe}/σ^{D} measured in [1], where σ^{Fe} and σ^{D} are the cross sections per nucleon for iron and deuterium respectively, showed deviations from unity which could not be interpreted in terms of the conventional prescription for Fermi motion. This effect (which is now generally referred to as the EMC effect) was subsequently confirmed by data from SLAC [2,3] and from the BCDMS collaboration at CERN [4]. The data show that the nuclear medium influences the deep inelastic scattering process. A recent account of the status of theoretical models of the effect can be found in [5].

The differential cross section per nucleon, for one photon exchange, can be expressed as follows

$$\frac{d^2\sigma^N}{dxdy} = \frac{8\pi\alpha^2 ME_\mu}{Q^4} F_2^N(x,Q^2) \left[1-y + \frac{y^2}{2[1+R^N(x,Q^2)]} \right].$$

In this expression $Q^2 = -q^2$, where q is the four momentum carried by the virtual photon. The usual Bjorken scaling variables are $x = Q^2/(2p_N.q) = Q^2/(2M\nu)$ and $y=(q.p_N)/(p.p_N) = \nu/E_\mu$, where p and p_N are the four momenta of the incident lepton and target nucleon respectively and M is the proton mass. The final expressions for x and y are the values in the frame where the target is at rest, and in this frame the energy transferred is ν and the incident lepton energy is E_μ. The cross sections depends on the nucleon structure function $F_2^N(x, Q^2)$ and on the ratio $R^N(x,Q^2) = \sigma_L(x,Q^2)/\sigma_T(x,Q^2)$; that is, the ratio of the longitudinal to transverse virtual photon cross sections.

Measurements of $R^N(x,Q^2)$ at high Q^2 [6], indicate that R^N is small and shows no strong dependence on the atomic number A of the target nucleus [7]. If R^N is independent of A, then the ratio of the cross sections per nucleon for different nuclei A_1 and A_2 is equal to the ratio of the structure functions per nucleon, $F_2^{A_1}/F_2^{A_2}$.

The original EMC data [1] were obtained from separate measurements of the absolute values of the nucleon structure function F_2 with iron and deuterium targets. These measurements were taken under different experimental conditions (beam energy, beam intensity, target arrangement and trigger) and at different times. In consequence, the systematic errors on the F_2^N ratios were rather large. In addition to the point-to-point systematic errors there was a further overall normalisation uncertainty of ± 7%.

In order to decrease the systematic errors, a new experiment was designed to measure directly the ratios of the nucleon structure functions from nuclear and deuterium targets. Thin targets of carbon, copper and tin and a liquid deuterium target were used. The geometry of the targets was similar and they were interchanged at intervals of a few hours in order to average out the effects of time dependent inefficiencies in the spectrometer and the beam intensity monitoring apparatus.

APPARATUS AND DATA TAKING

The experiment was performed in the M2 muon beam line at the CERN SPS using the EMC forward spectrometer to detect the scattered muons and the fast forward hadrons produced from deep inelastic scattering events. The data were taken in several experimental runs, with incident muon energies of 100, 120, 200 and 280 GeV.

Figure 1 shows a diagram of the apparatus. It was designed to measure simultaneously the spin dependent structure functions using a polarised target and the structure function ratios from the downstream targets. The nuclear and deuterium targets, each of thickness of $\sim 8\ g/cm^2$, were suspended from motor driven booms which allowed them to be interchanged frequently. The carbon, copper and tin targets were each in the form of 4 thin discs distributed over the same region in space as the 60 cm long deuterium target, in such a way that the acceptance was the same for each of the targets.

The forward spectrometer was similar to that described in [8] but modified to allow data to be taken at higher incident beam intensities than heretofore. To achieve this, the drift chambers upstream of the magnet described in [8] were replaced by the multiwire proportional chambers labelled PV1 and PV2 in fig. 1. Each of these chambers had the central region deadened to avoid backgrounds from the incident beam. Particles from deep inelastic scattering events in this region were detected by several small multiwire proportional chambers placed in the beam region which were specially designed to work in a high intensity environment. These chambers are labelled P0 in fig. 1.

DATA ANALYSIS

The raw data were passed through a chain of programs which performed pattern recognition and geometrical reconstruction of the incident and scattered muons, as well as any charged secondary hadrons which passed through the forward spectrometer magnet. A vertex fit, using the incident and scattered muons, was also performed. The flux of muons was determined using a random trigger [9].

In order to avoid regions of small or rapidly varying acceptance, or where radiative corrections were large, events were only accepted if they passed the selection criteria given in table 1. The cuts on y are such that the region at low x and high y, where radiative corrections are large, is thus avoided. The event yields were converted to cross sections using the measured muon flux and the appropriate target density and thickness. For the deuterium target a small correction (-1.4%) was made for events occurring in the mylar walls of the target. For the heavy nuclear targets a small correction (-0.9%) was made for events occurring in the air between the target discs. The cross section ratios measured from the various experimental runs agreed within errors and were combined in the subsequent analysis.

The measured ratios were corrected for radiative effects, so that they correspond to the single photon exchange diagram, following the procedures described in refs. [6] and [10]. The procedure includes corrections for the radiative tails of coherent elastic scattering from the nucleus and of quasi-elastic scattering from the nucleons (the latter includes a suppression at low Q^2 due to the Pauli Exclusion Principle), as well as corrections for deep-inelastic radiative scattering. The evaluation of the deep-inelastic radiative corrections requires knowledge of the absolute value of the structure functions, both inside and outside the kinematic domain of the data. The procedure adopted here was to use a parameterisation of the measured deuterium F_2^D values [10] and to evaluate F_2^A from this, using the measured structure function ratios. In this way most of the uncertainty in the radiative correction to the ratio due to the value of F_2^D in the unmeasured region is cancelled. The radiative corrections were then recalculated and the procedure iterated until convergence was obtained. In practice no significant variation persisted beyond the first iteration. It should be stressed that, after application of the kinematic cuts described in table 1, the correction factors applied to the cross section ratios are everywhere

small. The largest correction factor is at small x, and in the first x bin ($0.02 \leq x \leq 0.04$) the correction amounts to 3.1%, 7.6% and 11.4% for C/D, Cu/D and Sn/D respectively. The main part of the radiative correction which does not cancel in the ratios is from the coherent process. This term is calculated using parameterisations of the accurately measured nuclear form factors [11]. Uncertainties in the radiative correction procedure are included in the systematic errors, as discussed below.

The measured ratios were also corrected for the unequal numbers of protons and neutrons in the nuclear target. The correction was calculated using $F_2^n(x)/F_2^p(x) = (0.92-0.86x) \pm 0.05$, which is consistent with the available data [10].

RESULTS

The final corrected ratios of the nucleon structure functions obtained with C, Cu and Sn targets relative to those obtained with deuterium are given in table 2 and plotted in fig. 2. The ratios are extracted from the cross section ratios assuming $R^A = R^D$. The error bars shown in the figure are the total errors, obtained by adding the statistical and systematic errors in quadrature. The extent of the statistical errors is shown by the inner bars. As any variation with Q^2 of the ratios is relatively small the data from all Q^2 are combined for this analysis.

The systematic errors given in table 2 were calculated as follows. For each source of possible systematic error the contribution to the error on the ratio was calculated, separately for each bin of x and for each target ratio. These individual systematic errors were then added in quadrature to obtain the total estimated systematic error.

The main potential sources of systematic error are the following (a more detailed discussion can be found in ref. [12])

(i) Radiative corrections. In order to estimate this error the uncertainty in the measurements of the nuclear elastic form factors and in the size of the Pauli suppression factor were considered. Also included were the errors on the absolute value of F_2^D and on the ratio F_2^A/F_2^D, as well as that on $R^N(x)$. The combined uncertainties from these effects are largest for small values of x, and amount to 1.6%, 1.7% and 3.0% for the bin $0.02 \leq x < 0.04$ and to 1.1%, 1.2% and 1.3% for the bin $0.04 \leq x < 0.06$; for C/D, Cu/D and Sn/D respectively. For larger x this error is less than 1%.

(ii) Corrections for non-isoscalarity of the target. An error of ± 0.05 on $F_2^n(x)/F_2^p(x)$ was used in order to estimate the uncertainty on this correction. The correction is largest for Sn/D and amounts to $\pm$ 0.4% at small x, rising to $\pm$ 0.8% at large x.

(iii) Vertex selection criteria. The vertex distributions along the beam direction for deuterium and the heavy nuclear targets have a somewhat different shape because the deuterium target is continuous and the nuclear targets were discrete discs. Some uncertainty thus arises in the vertex selection because of the tails of the distributions and from background events. The possible error on the ratios due to this source was investigated both by Monte Carlo simulation and by studying the sensitivity of the ratios for different vertex cuts. The estimated error on the ratios F_2^A/F_2^D is $\pm$ 0.6%, and is independent of x.

(iv) Acceptance differences. The thicknesses in terms of radiation and interaction lengths of the various targets are different and hence the profiles of the hit distributions in the wire chambers, and potentially the reconstruction efficiencies, could be target dependent. This problem was investigated in two ways. Firstly a detailed Monte Carlo simulation of the experiment was carried out. Background hits were added by taking a real event in a similar kinematic region to the generated event, and from the same target, and adding all the hits, plane by plane, except those which had been successfully used by the reconstruction programs as belonging to a track. The second method consisted of comparing the event yields, after the usual selection criteria, in the polarised target (see fig. 1), in the presence of different heavy targets in the beam. No significant variation of the reconstruction efficiency with x was found within the systematic error ascribed for this effect, namely ± 1.5% for C/D and Cu/D and ± 2.7% for Sn/D.

In addition to the above errors there is an overall normalisation uncertainty (affecting all bins of x in the same way) amounting to ± 0.9% for each of the measured ratios. This error arises from the statistical error on the beam tracks accumulated to measure the muon flux [9], and on the uncertainties in the target masses.

The integrals

$$I^{A-D} = \int_{0.02}^{0.7} [F_2^A(x) - F_2^D(x)]dx$$

have been evaluated, and the results are shown in table 3. The value of $F_2^D(x)$ was taken from ref. [10] and the ratio $F_2^A(x)/F_2^D(x)$ was taken from table 2. The systematic error given was estimated by calculating the contribution to the integral I^{A-D} separately for each source of systematic error, then adding the resultant errors in quadrature. This integral represents the change in the momentum fraction carried by quarks and antiquarks. The results indicate a possible reduction in the visible momentum fraction per nucleon for heavy nuclei compared to that for deuterium.

DISCUSSION

The main features of the ratios of the nucleon structure functions F_2^A/F_2^D can be summarised as follows: There is a depletion below unity for values of $x \gtrsim 0.25$. The ratio is consistent with unity, or a small rise above unity in the x range roughly between 0.08 and 0.20. For small $x(\lesssim 0.05)$, the measured ratios lie below unity, and the magnitude of the deviation from unity grows with increasing atomic weight.

Taking into account the quoted statistical, systematic and overall normalisation errors, the measured ratios on Cu/D are compatible with the original measurements on Fe/D [1,10], except for a difference in the two lowest x points of 1-2 σ (fig. 3). The present data, extending lower in x, indicate a turning over of the ratio at low x. This effect becomes increasingly apparent at higher atomic weight.

A discussion of other experimental data on quark distributions in nuclei, and on the status of models for these effects, can be found in ref. [5]. Two main classes of models have emerged for the region $x \gtrsim 0.1$, namely the conventional nuclear physics models which involve a convolution of the contributions of the constituents (π, N,

Δ, multiquark bags etc.) of the nucleus and the Q^2 rescaling model. This latter model does not include the effects of Fermi motion and is applicable only for $x \lesssim 0.7$. Both these models can be expressed as a change in the scale of either x or Q^2 (or both) in nuclear matter. Empirically any model with such a scale change can be made to fit the existing data. Furthermore, the data suggest that the distance over which quarks move is larger for bound than for quasi-free nucleons.

None of the models in these categories can be used to describe the ratios observed at low values of x. The Vector Dominance Model (VDM) [13] partly describes nuclear shadowing phenomena for real photons and for low Q^2 and low x virtual photons. However, any VDM effects are predicted to fall off as $\sim 1/Q^2$, and so will have largely died out in the Q^2 range of this experiment. A possible explanation for shadowing at large Q^2 is the model of Nicolaev and Zakharov [14]. In this model the longitudinal extent $\Delta z \sim 1/Mx$ of the partons seen by the virtual photon is considered. For $x < x_c A^{-1/3}$, where $x_c \sim M_\pi/M_N \sim 0.15$, partons from different nucleons are within a common volume covering the whole nucleus in the longitudinal direction. Shadowing below x_c is attributed to the fusion of overlapping partons and, from momentum conservation, a rise in F_2^A/F_2^D above unity (antishadowing) is predicted in the region of $x \sim x_c$. This model does not explain the large x behaviour of the data, the physics of which may well modify the low x predictions of the model. However, the model is in qualitative agreement with the data except that it predicts a stronger A dependence than seen in the data. The Q^2- dependence of nuclear shadowing has been considered by Qiu [15] using modified Altarelli-Parisi equations which take into account parton recombination effects in nuclei. Qiu concludes that shadowing will vanish only slowly with increasing Q^2.

In summary, these investigations confirm previous observations that the nucleon structure functions for bound and quasi-free nucleons behave differently. The observed structure function ratio falls below

unity at large x ($\gtrsim$ 0.25), tends to rise above unity at medium x (~ 0.15) and then falls again below unity at small x ($\lesssim$ 0.05). In the small x region ($\langle Q^2 \rangle \sim 5$ GeV^2) this experiment shows evidence for nuclear shadowing similar to that observed at lower values of Q^2 at SLAC [16].

ACKNOWLEDGEMENTS

We would like to thank all people in the various laboratories who contributed to the construction, operation and analysis of this experiment. The support of the CERN staff in operating the SPS, muon beam and computer facilities is gratefully acknowledged.

REFERENCES

[1] EMC, J.J. Aubert et al., Phys. Lett. 123B (1983) 275.

[2] A. Bodek et al., Phys. Rev. Lett. 50 (1983) 1431;
A. Bodek et al., Phys. Rev. Lett. 51 (1983) 534.

[3] R.G. Arnold et al., Phys. Rev. Lett. 52 (1984) 727.

[4] BCDMS, G. Bari et al., Phys. Lett. 163B (1985) 282;
A.C. Benvenuti et al., Phys. Lett. 189B (1987) 483.

[5] E.L. Berger and F. Coester, ANL-HEP-PR-87-13 (to be published in Annual Review of Nuclear and Particle Science).

[6] EMC, J.J. Aubert et al., Nucl. Phys. B259 (1985) 189.
EMC, J.J. Aubert et al., Nucl. Phys. B272 (1986) 158.

[7] S. Dasu et al., University of Rochester preprint UR-991, ER 13065-479.

[8] EMC, O.C. Allkofer et al., Nucl. Inst. and Meth. 179 (1981) 445.

[9] R.P. Mount, Nucl. Inst. and Meth. 160 (1979) 23.

[10] EMC, J.J. Aubert et al., Nucl. Phys. B293 (1987) 740.

[11] J. Bailey et al., Nucl. Phys. B151 (1979) 367;
C.W. de Jager et al., Atomic Data and Nuclear Data Tables 14 (1974) 479;
J.R. Ficenec et al., Phys. Lett. 42B (1972) 213.

[12] V. Gibson, D. Phil. thesis, University of Oxford 1986, RAL-T.035;
M. Düren, Ph.D. thesis, III Physikalisches Inst. A, Aachen, 1987;
H. Cheung, D. Phil thesis, University of Oxford 1987.

[13] G. Grammer and J.D. Sullivan, in Electromagnetic Interactions of Hadrons, Vol.2 ed. by A. Donnachie and G. Shaw, Plenum (1978).

[14] N.N. Nikolaev and V.I. Zakharov, Phys. Lett. 55B (1975) 397.

[15] J. Qiu, Nucl. Phys. B291 (1987) 746.

[16] S. Stein et al., Phys. Rev. D12 (1975) 1884.

Table 1

Kinematic cuts applied to the data sample. The quantities p'_μ and θ_μ are the momentum and scattering angle respectively of the scattered muon.

Beam energy	100 & 120 GeV	200 GeV	280 GeV
$Q^2_{(min)}(GeV^2)$	2	3	3
$\nu_{(min)}(GeV)$	10	25	25
$p'_{\mu(min)}(GeV)$	20	30	40
$\theta_{\mu(min)}(mrad)$	10	10	10
$y \leq 0.65$ for $0.02 \leq x < 0.04$ $y \leq 0.75$ for $0.04 \leq x < 0.06$ $y \leq 0.85$ for $x \geq 0.06$			

Table 2

Values of the ratios of the structure functions per nucleon for a) carbon, b) copper and c) tin, compared to that for deuterium. In addition to the point-to-point systematic errors there are overall normalisation uncertainties of ±0.9%.

	$\langle x \rangle$	$\langle Q^2 \rangle$	F_2^A/F_2^D	stat. error	syst. error
a)	0.031	5.1	0.923	0.043	0.022
	0.050	7.8	1.020	0.035	0.020
	0.078	11.4	1.002	0.027	0.019
	0.123	14.4	1.044	0.032	0.019
	0.173	17.3	0.995	0.037	0.018
	0.243	20.2	0.957	0.032	0.018
	0.343	24.1	0.902	0.045	0.017
	0.442	29.8	0.902	0.069	0.017
	0.564	33.6	0.874	0.089	0.016
b)	0.031	4.4	0.940	0.026	0.023
	0.050	8.4	0.963	0.021	0.020
	0.079	13.5	0.997	0.017	0.019
	0.123	17.9	1.042	0.019	0.019
	0.173	21.1	1.018	0.023	0.019
	0.244	24.4	1.038	0.021	0.020
	0.342	29.5	0.945	0.029	0.018
	0.443	34.0	0.957	0.046	0.019
	0.573	40.4	0.897	0.061	0.018
c)	0.031	4.0	0.800	0.042	0.033
	0.050	7.7	0.873	0.037	0.027
	0.079	11.1	0.948	0.031	0.028
	0.123	14.6	1.008	0.037	0.030
	0.173	17.1	1.030	0.044	0.031
	0.246	19.8	1.009	0.041	0.030
	0.343	24.8	0.927	0.056	0.028
	0.443	32.4	0.841	0.083	0.026

Table 3

Values of the integral I^{A-D} for different targets

Target Combination	x region	$I^{A-D} \times 10^3$		
		value	stat. err.	syst. err.
C/D	0.02-0.7	-4.7 ±	1.8 ±	2.3
Cu/D	0.02-0.7	-1.2 ±	1.2 ±	2.3
Sn/D	0.02-0.7	-3.6 ±	2.4 ±	3.5

FIGURE CAPTIONS

Fig. 1 Schematic diagram of the EMC forward spectrometer used to measure the polarised target asymmetries and the structure function ratios from various nuclear targets.

Fig. 2 Ratios of the nucleon structure functions a) F_2^C/F_2^D, b) F_2^{Cu}/F_2^D and c) F_2^{Sn}/F_2^D as a function of x. The ratios are extracted from the cross sections assuming $R^A = R^D$, and are corrected for radiative effects. The errors shown are the total errors, obtained by adding the statistical and systematic errors in quadrature. The extent of the statistical errors is shown by the inner bars.

Fig. 3 Ratios of the nucleon structure functions F_2^{Cu}/F_2^D (this experiment) - full circles, F_2^{Fe}/F_2^D [10] - full squares (inner errors are statistical, outer are total i.e. combined statistical and systematic), F_2^{Fe}/F_2^D [4] - open circles and F_2^{Fe}/F_2^D [2,3] - open triangles. The error bars shown are the total errors, obtained by adding the statistical and systematic errors in quadrature.

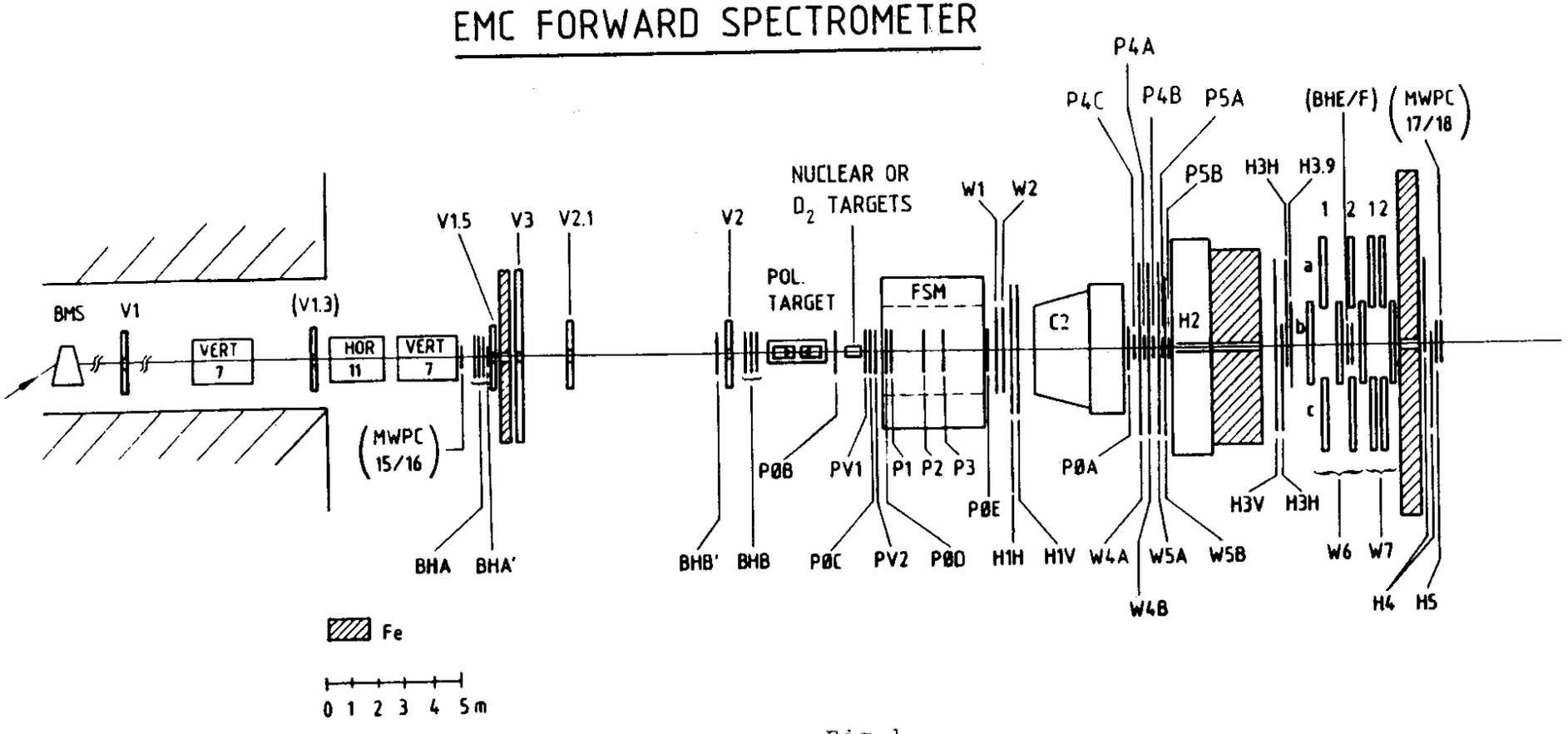
EMC FORWARD SPECTROMETER
BMS
V1
(V1.3)
VERT 7
HOR 11
VERT 7
V1.5
V3
V2.1
V2
NUCLEAR OR D_2 TARGETS
POL. TARGET
FSM
W1
W2
C2
P4A
P4C
P4B
P5A
P5B
H2
H3H
H3.9
(BHE/F)
(MWPC 17/18)
1
2
1 2
a
b
c
(MWPC 15/16)
BHA
BHA'
BHB'
BHB
PØB
PV1
P1
P2
P3
PØE
PØA
PØC
PV2
PØD
H1H
H1V
W4A
W4B
W5A
W5B
H3V
H3H
W6
W7
H4
H5
Fe
0 1 2 3 4 5 m

Fig.1

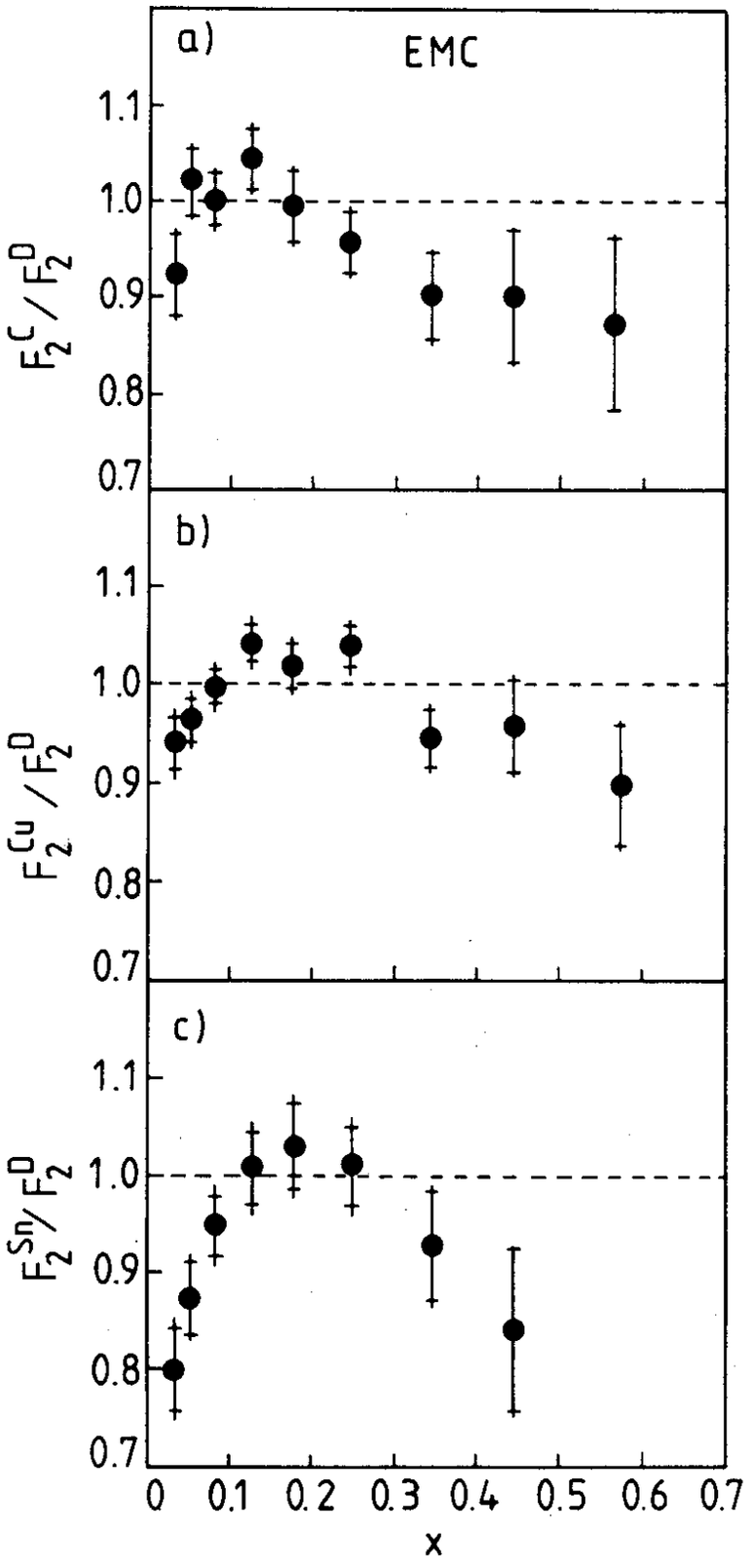
a)
EMC
b)
c)
F_2^C / F_2^D
F_2^{Cu} / F_2^D
F_2^{Sn} / F_2^D
1.1
1.0
0.9
0.8
0.7
0
0.1
0.2
0.3
0.4
0.5
0.6
0.7
x

Fig.2

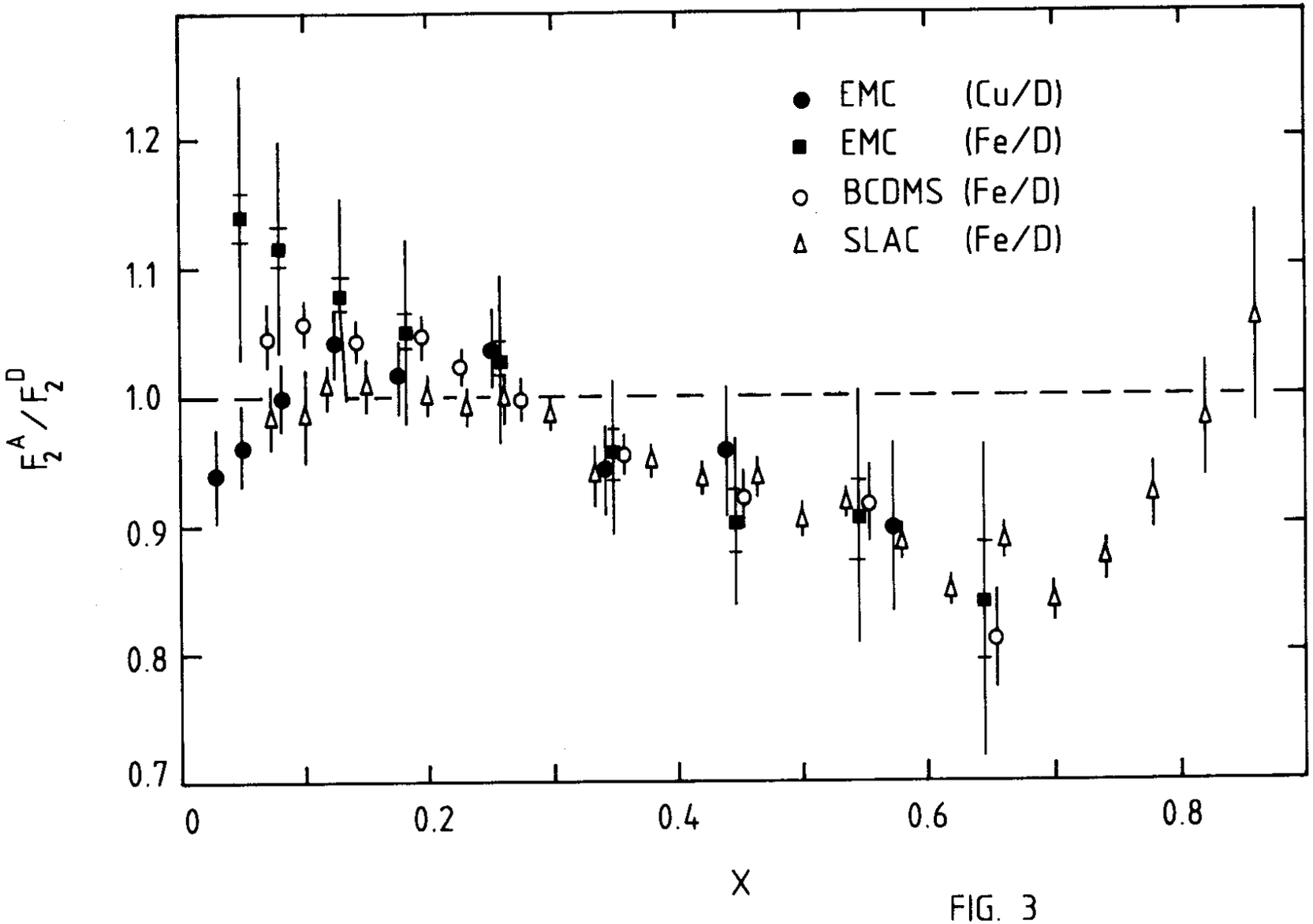
EMC (Cu/D)
EMC (Fe/D)
BCDMS (Fe/D)
SLAC (Fe/D)
F_2^A / F_2^D
1.2
1.1
1.0
0.9
0.8
0.7
0
0.2
0.4
0.6
0.8
X

FIG. 3